Available online at www.sciencedirect.com

SciVerse ScienceDirect

Ceramics International 38 (2012) 5999–6007

CERAMICS INTERNATIONAL

www.elsevier.com/locate/ceramint

Interaction of chitosan with tetraethyl orthosilicate on the formation of silica nanoparticles: Effect of pH and chitosan concentration

Thongthai Witoon [a,b,*], Metta Chareonpanich [a,b]

[a] National Center of Excellence for Petroleum, Petrochemicals and Advance Material, Department of Chemical Engineering, Faculty of Engineering, Kasetsart University, Bangkok 10900, Thailand

[b] Center for Advanced Studies in Nanotechnology and Its Applications in Chemical Food and Agricultural Industries, Kasetsart University, Bangkok 10900, Thailand

Received 5 March 2012; received in revised form 5 April 2012; accepted 18 April 2012
Available online 26 April 2012

Abstract

In this paper, we report the interaction of chitosan with tetraethyl orthosilicate on the formation of silica nanoparticles under different conditions of pH (5–9) and chitosan concentration (0–0.001379 mM). The silica nanoparticles were characterized by means of N_2-sorption, scanning electron microscopy and transmission electron microscopy. It was found that chitosan played two different roles on the formation of silica nanoparticles, depending on the pH values. At a low chitosan concentration, chitosan promoted the formation of larger silica nanoparticles in the pH range of 5–6, while it reduced the size of silica nanoparticles when the pH value was increased to the range of 6.5–8.5. However, based on the results of N_2-sorption analysis, two different sizes of silica nanoparticles caused by the growth of silica at different phases were observed. At high chitosan concentration, the size of silica nanoparticles continuously increased in the pH range of 5–6, while only smaller size of silica nanoparticles was obtained in the pH range of 6.5–8.5. At pH 9, chitosan molecules were found to have no significant effect on the formation of silica nanoparticles even though a large amount of chitosan was employed.

Keywords: A. Powder: chemical preparation; B. Porosity; D. SiO_2; Chitosan

1. Introduction

Silica materials have attracted much attention from researchers because of their commercial applications as catalyst supports, in controlled drug release, and as sorbents [1–3]. Over the past two decades, there has been an increasing interest in the synthesis of various porous silicas by using organic materials as additives in order to fully control the entire pore system as it ranges from micropores to macropores. Recently, several kinds of biopolymer containing amine functionalities have attracted much interest for the synthesis of silica materials because they enable the formation of silica nanoparticles under environmentally friendly conditions, and moreover, silica can possibly mimic their morphology [4]. Patwardhan et al. [4] pointed out that there are three main roles of amine-based polymers in the synthesis of silica materials: (1) catalysis, (2) aggregation, and (3) structure direction (template/scaffold) or a combination thereof. Indeed, silicatein extracted from the sponge *Tethya aurantia* was found to enhance the hydrolysis and condensation of silicic acid at neutral pH [5]. Cationic peptides, including poly-L-lysine and poly-L-arginine were found to dramatically promote the aggregation of silica due to electrostatic or chemical interactions [6]. In addition, poly-L-lysine was found to direct the formation of spherical, petal-like and sheet-like hexagonal silica [7]. Due to the fact that synthetic amine-based polymers from natural biosilica sources cannot be readily obtained restricting their industrial applications. Therefore, the invention on bioinspired silica synthesis should not be limited to understanding their roles in the formation of silica products, but should also extend to the use of biomaterials that are cheaper and readily available in nature.

Recently, it has been demonstrated that chitosan, which is produced from partial *N*-deacetylation of chitins, easily obtained from a commercial source, is effective for bioinspired

* Corresponding author at: National Center of Excellence for Petroleum, Petrochemicals and Advance Material, Department of Chemical Engineering, Faculty of Engineering, Kasetsart University, Bangkok 10900, Thailand. Tel.: +66 2579 2083; fax: +66 2561 4621.
E-mail address: fengttwi@ku.ac.th (T. Witoon).

0272-8842/$36.00
http://dx.doi.org/10.1016/j.ceramint.2012.04.056

silica synthesis at ambient temperature and neutral pH. However, to the best of our knowledge, the effect of chitosan on the formation of silica nanoparticles has not yet been understood. Moreover, different roles of chitosan molecules on the formation of silica nanoparticles have been reported. For example, Chang et al. [8] found that chitosan could catalyze the aggregation of colloidal silica nanoparticles in weakly acidic solution (pH values of 4–5.6) without a significant increase in the rate of silica polycondensation. Demadis et al. [9] revealed that phosphonated chitosan was able to inhibit silicic acid condensation at neutral pH *via* a combination of electrostatic and hydrogen-bonding interactions. Our previous work reported the effect of chitosan on the formation of silica particles using sodium silicate derived from rice husk ash as a silica source [10–12]. We found that chitosan played an important role as a scaffold for the biosilica deposition, leading to the formation of the bimodal porous silicas after chitosan removal. The different roles of chitosan molecules might result from the different investigated conditions such as pH value, temperature, concentration and type of precursors.

In this study, we report the effects of pH and chitosan concentration on silica synthesis using tetraethyl orthosilicate (TEOS) as a silica source (instead of sodium silicate). N_2-sorption was used to determine the pore size and the size of the silica nanoparticles, while scanning electron microscopy (SEM) and transmission electron microscopy (TEM) were used to investigate the morphology and size of silica nanoparticles. Based on the results of our analyses we found that chitosan molecules could control the size of silica nanoparticles; to better understand the process, a model for this bioinspired silica synthesis was proposed. These results provide essential information for further development of a simple, low-cost, environmentally friendly route to synthesize silica with novel structures and tailored properties.

2. Experimental

2.1. Chemicals and reagents

Chitosan with 80% deacetylation was purchased from Eland Corporation. The molecular weight of the chitosan, determined by Gel Permeation Chromatography (GPC, Waters 600E) using 0.5 M acetic acid and 0.5 M sodium acetate as the eluent was found to be approximately 290 kDa. Tetraethyl orthosilicate (TEOS), acetic acid and ammonium hydroxide were purchased from Sigma–Aldrich. All chemicals and reagents are of analytical grade and used without any further purification.

2.2. Preparation of silica nanoparticles

In a typical synthesis process, chitosan was dissolved overnight in 60 mL of 2% (v/v) acetic acid in deionized water at room temperature, agitated with a magnetic stirrer overnight. Subsequently, TEOS was added into the chitosan solution. It should be noted that, measured with a pH meter (model CG-842, Schott), the pH value after mixing was approximately 4. Then the pH value of the mixture was quickly adjusted to 5, 6, 6.5, 7, 8.5, and 9 by the addition of 5 M NH_4OH. The resulting mixtures, containing SiO_2 (0.015625 M) and chitosan (0, 0.000345, and 0.001379 mM), were stirred at 40 °C for 6 h. Subsequently, the obtained mixtures were transferred into a glass bottle and aged in an oven at 60 °C for 24 h. The resulting products were obtained by washing with deionized water, followed by three centrifugation/redispersion cycles at 10,000 rpm for 10 min. The silica–chitosan composites were dried at 120 °C for 24 h and calcined in air at 600 °C for 4 h at a heating rate of 2 °C/min. The obtained products are designated as S-*X*-*Y* where *X* is the pH value and *Y* is the chitosan concentration.

2.3. Characterization of porous silica products

Nitrogen sorption isotherms of silica products were measured at −196 °C with a Quantachrome Autosorb-1C instrument. Prior to sorption measurements, the products were degassed at 200 °C for 12 h. The pore size distribution was calculated by using the Barrett–Joyner–Halenda (BJH) methods. The specific pore volumes were measured at a relative pressure P/P_0 of 0.995. The total surface area (S_{BET}) of the silica products was derived by using the BET (Brunauer–Emmert–Teller) analysis in the relative pressure range between $P/P_0 = 0.05$ and 0.3. In order to determine the envelope surface area of only the backbone particles, the so-called specific external surface area S_{ext} was estimated as the difference between S_{BET} and S_{micro}, where S_{micro} was the micropore surface area determined by a modified *t*-plot method (MP-method). The mean particle size *d* was related to the specific external surface area and the particle density by Alexander and Iler [13]

$$d = \frac{6}{S_{ext} \cdot \rho_{silica\ particle}} \quad (1)$$

where the density of a silica nanoparticles was assumed to be 2200 kg/m^3 [13].

The surface morphology of the silica products was analyzed with a field emission scanning electron microscopy (FE-SEM: JEOL JSM-6301F with Au-coating, operated at 20 keV). The nanostructures of the products were revealed with the application of transmission electron microscopy (TEM: JEOL JEM-2010 microscope with an acceleration voltage of 200 kV). In order to prepare a sample for TEM analysis, the porous silica products were suspended in ethanol and dried at room temperature on a copper grid coated with a carbon film.

3. Results and discussion

Fig. 1 shows the N_2-sorption isotherm of the calcined silica products prepared at different pH values and chitosan concentrations. Without the use of chitosan, the isotherm of silica products synthesized at pH 5 shows a typical type IV shape with H2 hysteresis loop (Fig. 1a), indicating an ink-bottle pore structure. When the pH of the mixture was increased from 5 to 6.5, the isotherms shifted toward higher relative pressure

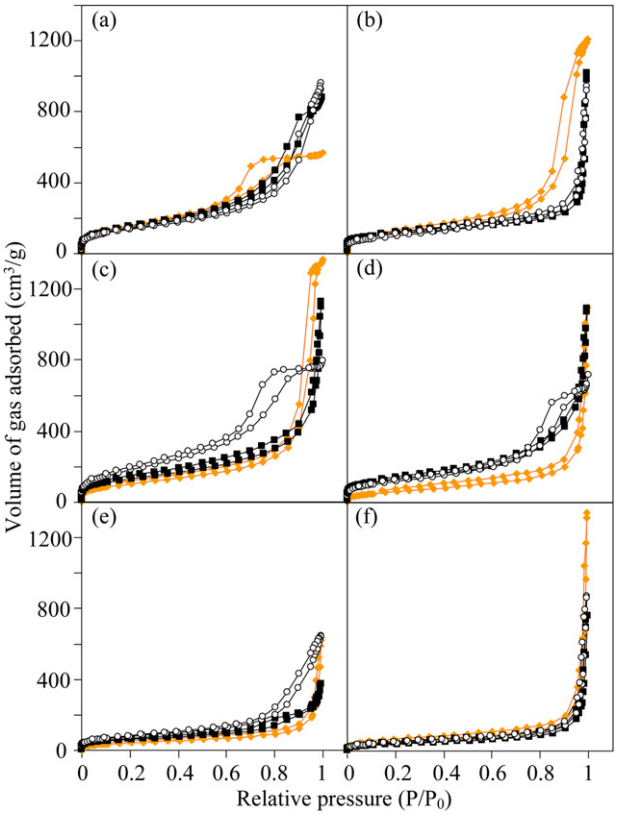

Fig. 1. N_2 sorption isotherms of silica products prepared at different pH values and chitosan concentrations: (a) pH 5, (b) pH 6, (c) pH 6.5, (d) pH 7, (e) pH 8.5 and (f) pH 9. The symbols orange diamond, black rectangular and white cycle represent the products without chitosan, with 0.000345 mM chitosan, and with 0.001379 mM chitosan, respectively. (For interpretation of the references to color in this figure legend, the reader is referred to the web version of the article.)

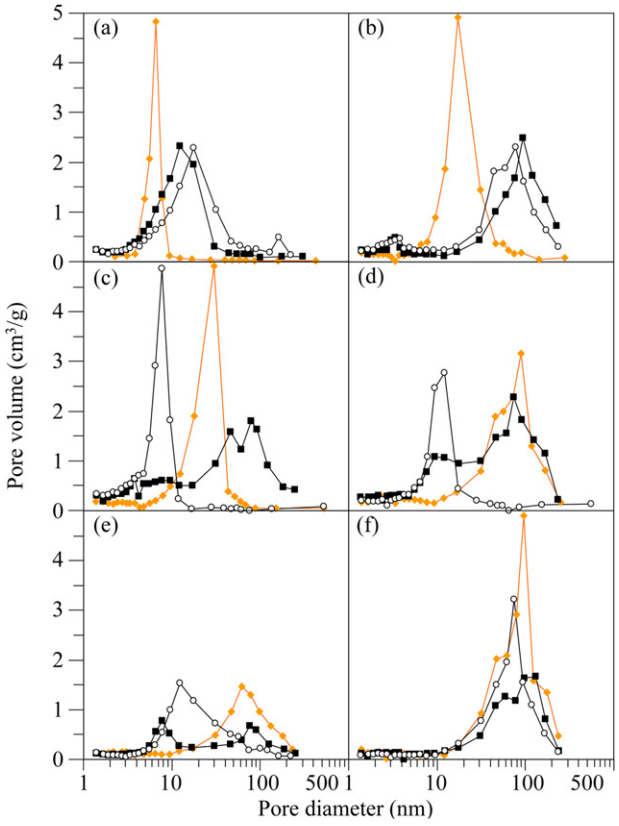

Fig. 2. Pore size distribution of silica products prepared at different pH values and chitosan concentrations: (a) pH 5, (b) pH 6, (c) pH 6.5, (d) pH 7, (e) pH 8.5, and (f) pH 9. The symbols orange diamond, black rectangular and white cycle represent the products without chitosan, with 0.000345 mM chitosan, and with 0.001379 mM chitosan, respectively. (For interpretation of the references to color in this figure legend, the reader is referred to the web version of the article.)

and the type of hysteresis loop was changed to H1, indicating the existence of pores in the form of interstices between closed-packed and equal-sized spherical particles. With yet higher pH values, the type IV isotherm was no longer obtained and instead a type II isotherm was observed, an indication of the presence of macropores. Once chitosan was applied, the isotherm types and hysteresis loops were significantly changed depending on both the pH of mixture and the chitosan concentration. The isotherms were however not clear enough to reveal the effect of the pH of mixture and chitosan concentration on the size of silica particle. As a result, the pore size distribution, SEM, and TEM images of silica products are employed instead.

The pore size distributions of the silica products synthesized at various conditions are shown in Fig. 2. It was found that the effect of chitosan addition at different pH values of the mixture can be classified into three categories: (1) increased pore size ($5 \leq pH \leq 6$), (2) decreased pore size ($6.5 \leq pH \leq 8.5$), and (3) no effect on the pore size (pH 9). For the first category, the pore size is affected by the different levels of chitosan concentration. For the second category, the silica products prepared at low chitosan concentration exhibited a bimodal pore size distribution, whereas only smaller pore sizes existed in the silica products prepared at a higher chitosan concentration. The physical properties of all silica products are given in Table 1. The average particle size of the silica products (Fig. 3) was evidently found to correspond to their pore sizes. However, the average particle size of the silica products prepared at pH 6.5 and low chitosan concentration was larger than that prepared at same pH but without the chitosan addition. This can be explained by the fact that two different silica particle sizes of silica products were obtained with mainly large silica nanoparticles.

The surface morphologies of the silica products were investigated by SEM and representative images are shown in Fig. 4. At pH 5, the silica product prepared without chitosan

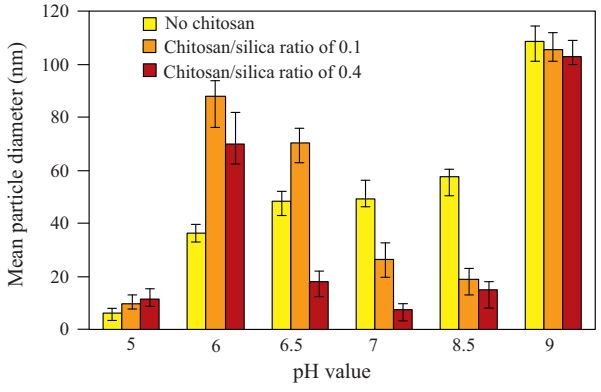

Fig. 3. Average size of silica particles determined by N_2-sorption.

Table 1
Physical properties of the products synthesized under various conditions.

Sample ID[a]	BET surface area (m^2/g)	Micropore surface area (m^2/g)	External surface area (m^2/g)	Average silica particle size (nm)	Total pore volume (cm^3/g)
S-5-0	574	117	457	6.0	0.88
S-5-0.000345	535	247	288	9.5	1.37
S-5-0.001379	483	247	236	11.5	1.49
S-6-0	426	345	81	33.6	1.67
S-6-0.000345	370	339	31	88.0	1.87
S-6-0.001379	351	312	39	70.1	1.66
S-6.5-0	410	353	57	48.3	2.26
S-6.5-0.000345	497	458	39	70.3	1.66
S-6.5-0.001379	730	578	152	18.0	1.56
S-7-0	230	175	55	49.2	1.70
S-7-0.000345	445	342	103	26.5	2.04
S-7-0.001379	420	56	364	7.5	1.32
S-8.5-0	150	102	48	57.4	0.98
S-8.5-0.000345	277	133	144	18.9	0.78
S-8.5-0.001379	207	26	181	15.0	1.00
S-9-0	195	170	25	108.7	2.08
S-9-0.000345	146	120	26	105.3	1.55
S-9-0.001379	160	133	27	103.0	1.68

[a] The silica products are designated as S-*X*-*Y* where *X* is the pH value and *Y* is the chitosan concentration.

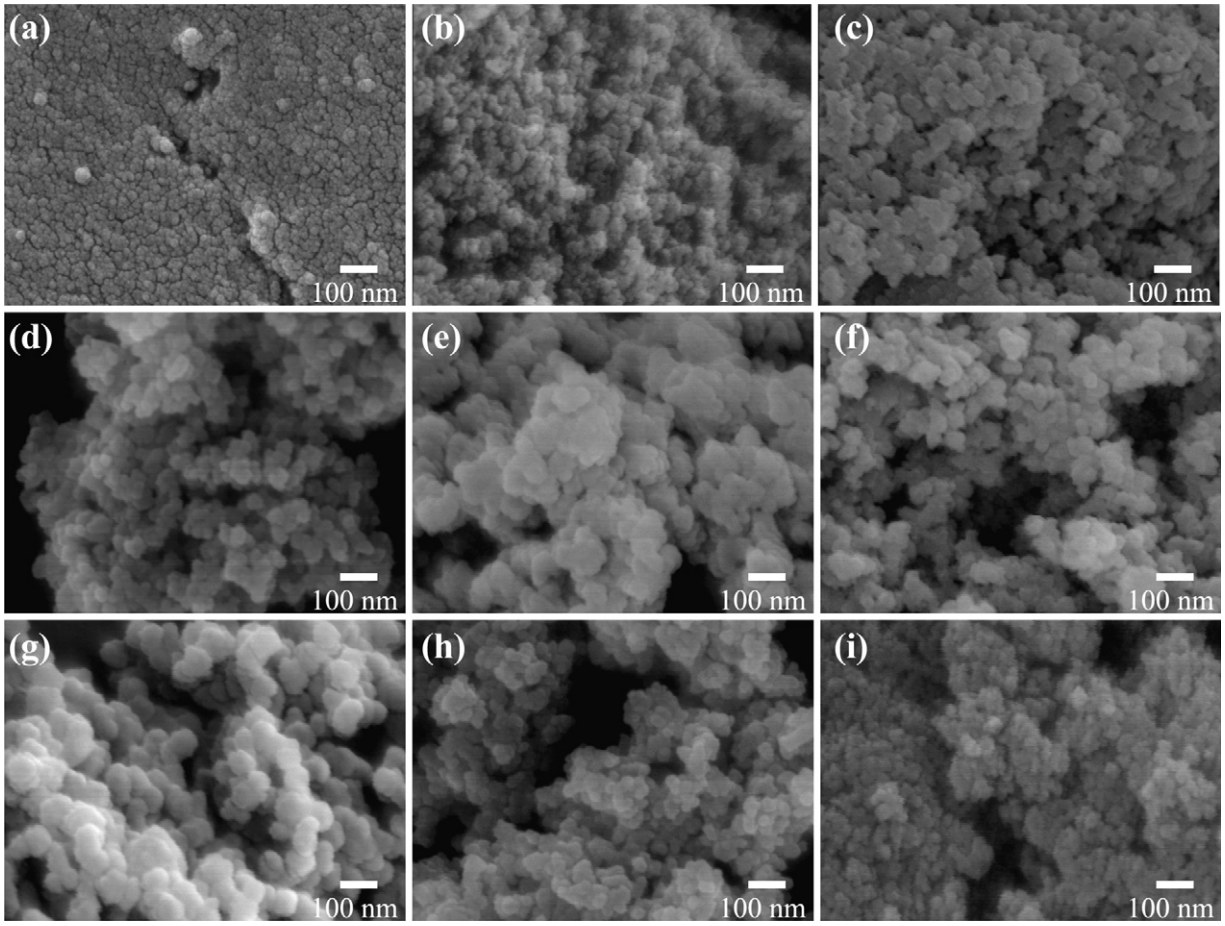

Fig. 4. SEM images of silica products prepared at different pH values and chitosan concentrations: (a) pH 5 and w/o chitosan, (b) pH 5 and 0.000345 mM chitosan, (c) pH 5 and 0.001379 mM chitosan, (d) pH 6.5 and w/o chitosan, (e) pH 6.5 and 0.000345 mM chitosan, (f) pH 6.5 and 0.001379 mM chitosan, (g) pH 7 and w/o chitosan, (h) pH 7 and 0.000345 mM chitosan, and (i) pH 7 and 0.001379 mM chitosan.

(Fig. 4a) showed a dense and continuous gel with an aggregate size of approximately 20 nm. With increasing chitosan concentration (Fig. 4b and c), the surface morphology changed to a loose aggregate of silica nanoparticles (30–50 nm). At pH 6.5 (Fig. 4d–f) the silica product prepared without chitosan (Fig. 4d) showed a loose aggregate of silica nanoparticles with an average size of approximately 50 nm. Moreover, the size of silica nanoparticle first increases and then decreases when the chitosan concentration is increased from 0.000345 to 0.001379 mM. The surface morphology of silica products prepared at pH 7 (Fig. 4g–i) showed the opposite trend of the morphology of silica products prepared at pH 6.

TEM was performed to reveal the size of silica nanoparticles; representative images of silica products prepared at pH 5 and 7 are shown in Figs. 5 and 6, respectively. At pH 5 and no chitosan addition (Fig. 5a and b), the size of silica nanoparticles was approximately 5–7 nm. The size of silica nanoparticles was increased from 10–12 nm (Fig. 5c and d) to 14–18 nm (Fig. 5e and f) with increasing chitosan concentration. At pH 7, the size of silica nanoparticles prepared without the chitosan was approximately 20–36 nm (Fig. 6a and b). At low chitosan concentration (Fig. 6c and d), the silica product consisted of two different domains, the aggregate of large and small sizes of silica nanoparticles. At high chitosan concentration (Fig. 6e and

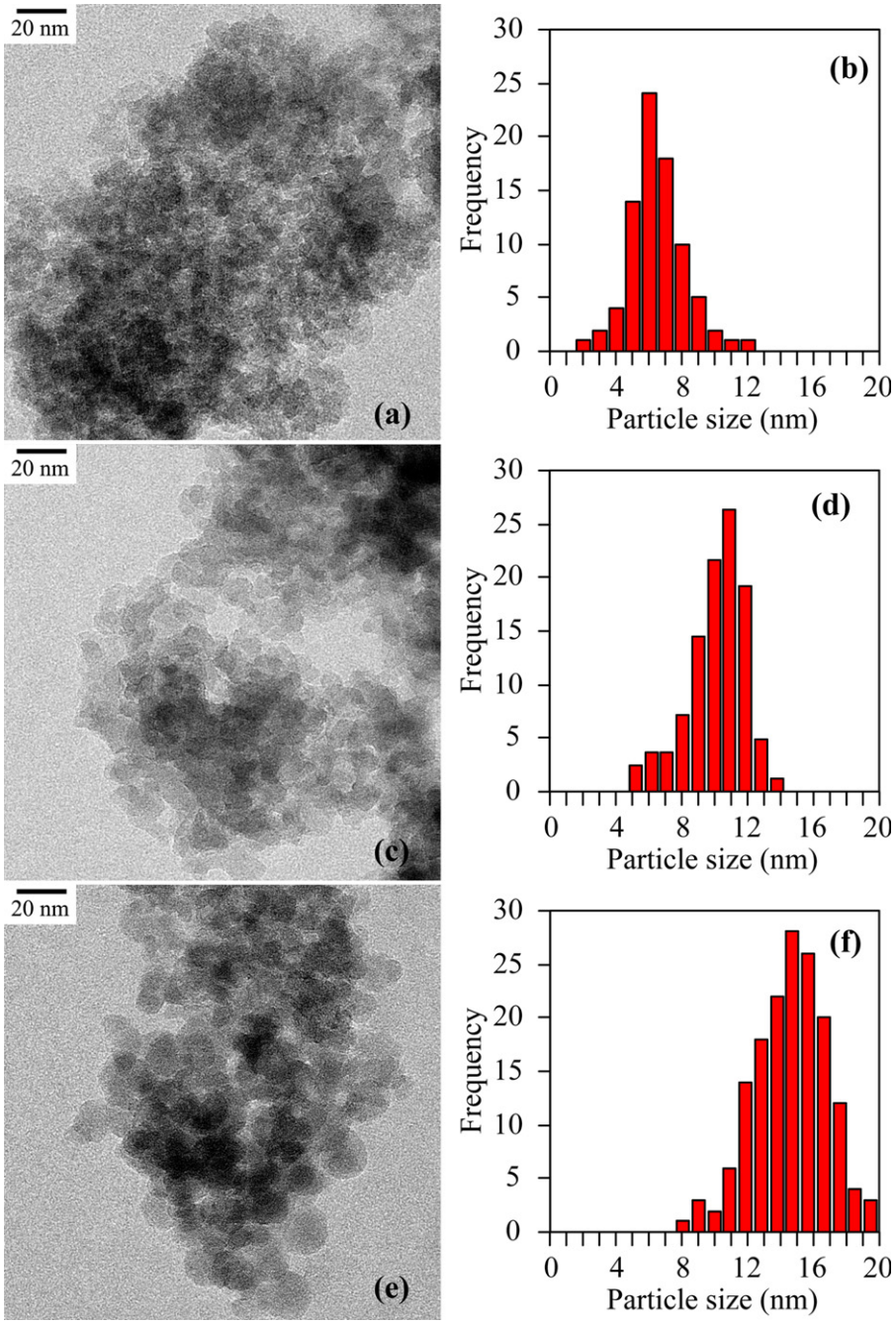

Fig. 5. TEM images and histogram analysis of silica products prepared at pH 5 and different chitosan concentrations: (a) and (b) w/o chitosan, (c) and (d) 0.000345 mM chitosan, (e) and (f) 0.001379 mM chitosan.

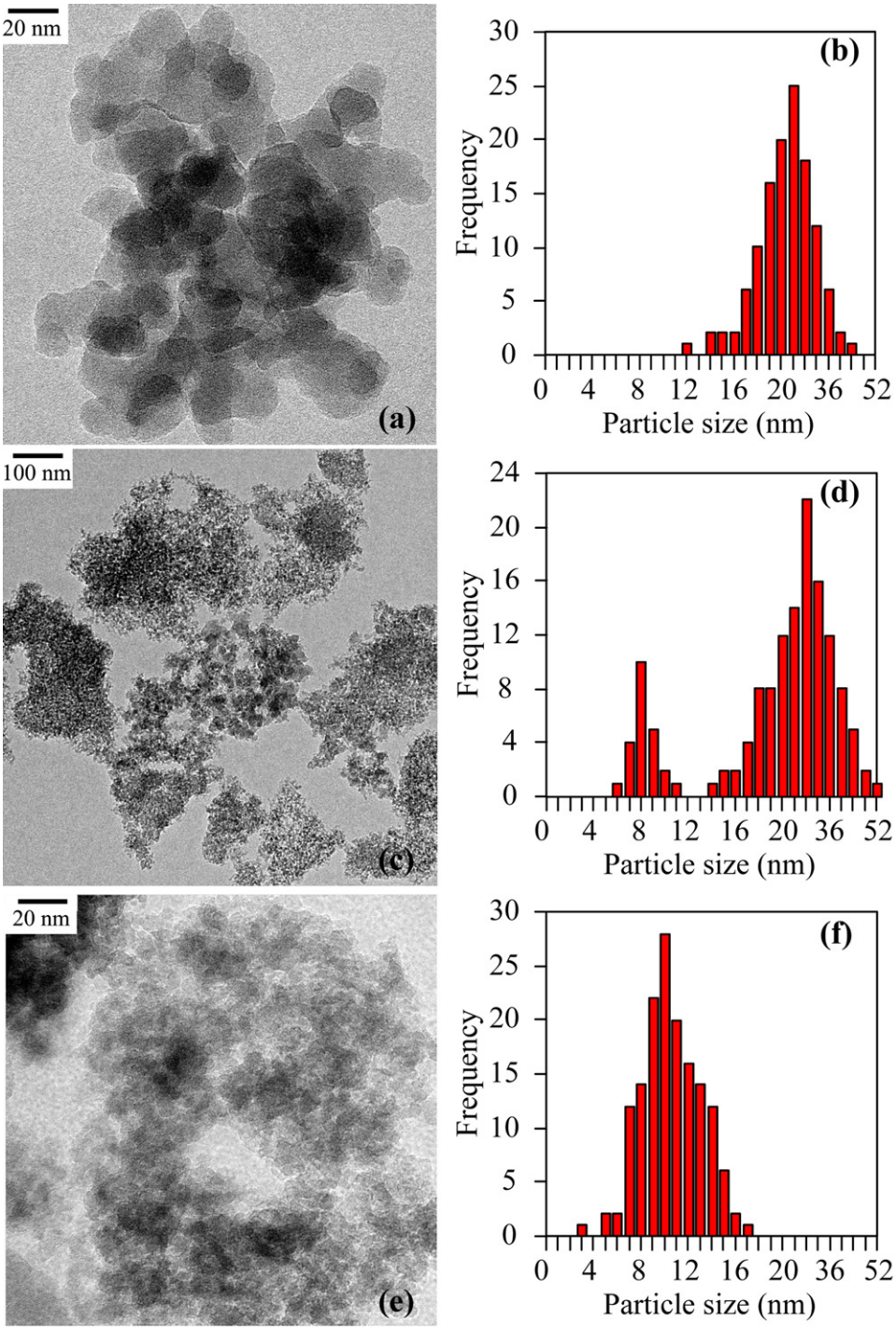

Fig. 6. TEM images and histogram analysis of silica products prepared at pH 7 and different chitosan concentrations: (a) and (b) w/o chitosan, (c) and (d) 0.000345 mM chitosan, (e) and (f) 0.001379 mM chitosan.

f), the aggregation of large-sized silica particles was no longer observed and instead the aggregation of small-sized silica particles was found. The results from TEM analysis are in good agreement with the results of N_2-sorption.

The formation mechanisms of silica products prepared at different pH values and chitosan concentrations are proposed as shown in Fig. 7. Based on the results mentioned above, it was found that chitosan plays two different roles in the growth of silica particles depending on the range of pH values: (1) at pH 5–6, chitosan promotes the increase of silica particle size and (2) at pH 6.5–8.5, chitosan decreases the size of silica particle. Many works have reported that the amino groups along the backbone chains of polymers can act as an acid–base catalyst that facilitates the rate of silica condensation [5,14]. The increase of silica condensation rate results in a highly branched structure; this in turn prevents the shrinkage of silica at an earlier state of drying due to the stiffness of the impinging clusters, resulting in larger pores

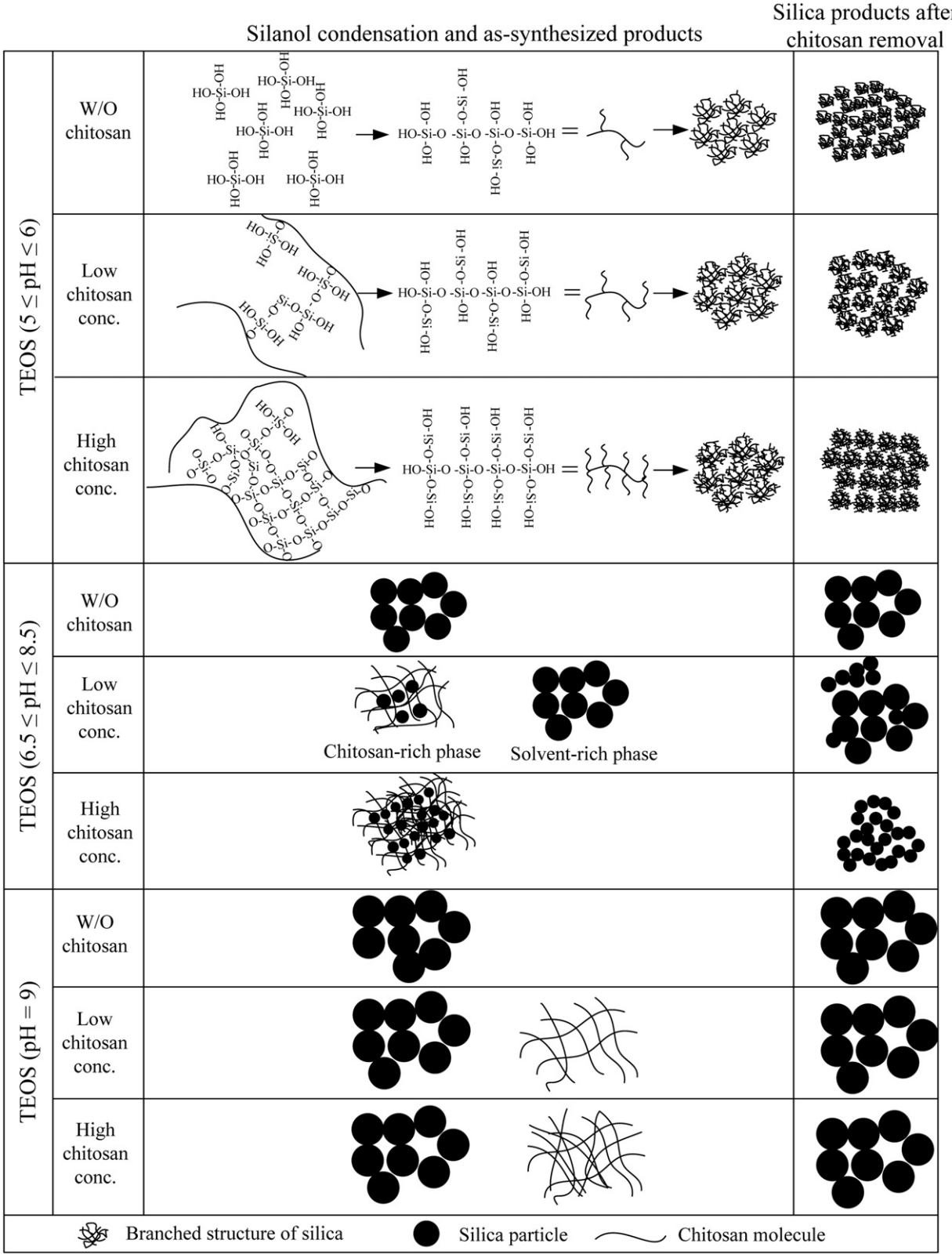

Fig. 7. Schematic presentation of the roles of chitosan on the silica formation at different pH values and chitosan concentrations.

[15]. This provides a reasonable explanation for the effect of chitosan molecules on the growth of the silica nanoparticles at pH $\leq$ 6. However, it fails to explain why the size of the silica nanoparticle tends to decrease when the pH of the mixture is varied in the range of 6.5 and 8.5. Moreover, the results of pore size distribution (Fig. 2) and TEM image (Fig. 6c and d) indicated that there are two different sizes of silica nanoparticle occurring at a low chitosan concentration.

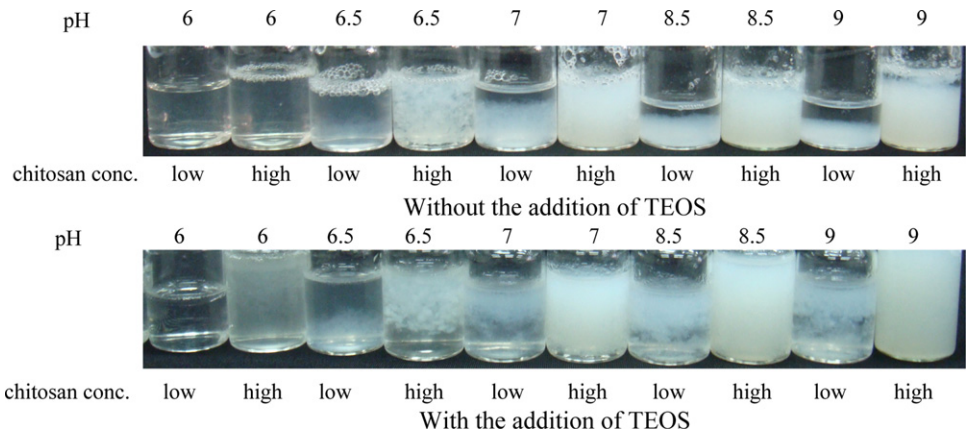

Fig. 8. Visual observations of the chitosan solution and TEOS–chitosan solution at different pH values and chitosan concentrations.

This was possibly attributed to the dissimilarity of the growth of silica nanoparticles.

Visual inspection of the chitosan precipitates at different pH values and chitosan concentrations gives valuable information and is useful to explain the effects of chitosan on the formation of silica nanoparticles at $6.5 \leq \text{pH} \leq 8.5$ (Fig. 8). It can be seen that the initial chitosan in a 1% (v/v) acetic acid solution had a very clear appearance (pH value of approximately 4). The pH value of the chitosan solution was adjusted by using 5 M NH_4OH. At pH 5 and 6, the solution remained clear at all chitosan concentrations. Once the pH value was adjusted to 6.5, the chitosan immediately precipitated and the amount of precipitate increased with increasing chitosan concentrations. A similar trend was also found in the pH range of 6.5–9. This observation could be explained by the fact that the chitosan has a pK_a value of ~6.5, and therefore it could be dissolved in the acidic solution due to the protonation of amino groups. The increase in pH value caused a decrease in the number of these positively charged amino groups, resulting in the aggregation and precipitation of chitosan molecules (phase separation).

Adding TEOS into the chitosan solution and adjusting the pH of the mixture gave a similar result to the original chitosan solution (Fig. 8). When TEOS was hydrolyzed to silicic acid in a low chitosan concentration system, it could distribute into a solvent-rich phase and a chitosan-rich phase. The silica growth in the solvent-rich phase was therefore similar to the silica synthesized without the addition of chitosan (see Fig. 2c–e). Based on the results of the pore size distribution of silica products synthesized without the chitosan, the size of silica nanoparticles in the solvent-rich phase was larger than that in the chitosan-rich phase. One possible explanation is that chitosan molecules can react with silicic acid through residual protonation of amino groups or through hydrogen-bonding with hydroxyl groups [8,16], which not only reduce the quantity of available silicic acid but also prevent further silica condensation reactions. Additionally, the size of silica nanoparticles might be limited by the size of the chitosan network, resulting in the occurrence of smaller silica nanoparticles. As results, the silica products synthesized at low chitosan concentration have two different sizes. At a higher chitosan concentration, almost all of the silicic acid reacted with chitosan molecules, and therefore, only small silica nanoparticles could be formed.

4. Conclusion

In summary, the interaction of biopolymer chitosan with tetraethyl orthosilicate on the formation of silica nanoparticles was explored at various pH values of the mixture and at various chitosan concentrations. For $5 \leq \text{pH} \leq 6$ and low chitosan concentration, the size of silica nanoparticles significantly increased due to the enhancement of the rate of silica condensation. The size of the silica nanoparticles had significant dependence on chitosan concentration. For $6.5 \leq \text{pH} \leq 8.5$ and low chitosan concentration, a bimodal pore size distribution was obtained since silica grew in two distinct phases. When chitosan concentration was increased yet further, only small silica particle sizes were observed. However, at pH 9, chitosan did not show any significant effect on the formation of silica products. The results presented here contribute to understanding of how chitosan molecules control silica synthesis, as well as the novel development methods of materials with tailored properties.

Acknowledgements

This work is financially supported by the Research Grant for New Scholar (Grant No. MRG5480196) co-funded by the Thailand Research Fund (TRF); the Commission on Higher Education, Thailand; and Kasetsart University, Thailand. Support from the ‘‘National Research University Project of Thailand (NRU)’’ is also acknowledged.

References

[1] T. Witoon, M. Chareonpanich, J. Limtrakul, Effect of hierarchical meso–macroporous silica supports on Fischer–Tropsch synthesis using cobalt catalyst, Fuel Processing Technology 92 (2011) 1498–1505.
[2] F. Chen, Y. Zhu, Chitosan enclosed mesoporous silica nanoparticles as drug nano-carriers: sensitive response to the narrow pH range, Microporous and Mesoporous Materials 150 (2012) 83–89.
[3] T. Witoon, N. Tatan, P. Rattanavichian, M. Chareonpanich, Preparation of silica xerogel with high silanol content from sodium silicate and

its application as CO_2 adsorbent, Ceramics International 37 (2011) 2297–2303.
[4] S.V. Patwardhan, S.J. Clarson, C.C. Perry, On the role(s) of additives in bioinspired silicification, Chemical Communications (2005) 1113–1121.
[5] Y. Zhou, K. Shimizu, J.N. Cha, G.D. Stucky, D.E. Morse, Efficient catalysis of polysiloxane synthesis by silicatein α requires specific hydroxyl and imidazole functionalities, Angewandte Chemie-International Edition 38 (1999) 779–782.
[6] T. Coradin, O. Durupthy, J. Livage, Interactions of amino-containing peptides with sodium silicate and colloidal silica: a biomimetic approach of silicification, Langmuir 18 (2002) 2331–2336.
[7] S.V. Patwardhan, N. Mukherjee, M. Steinitz-Kannan, S.J. Clarson, Bioinspired synthesis of new silica structures, Chemical Communications (2003) 1122–1123.
[8] J.S. Chang, Z.W. Kong, D.F. Hwang, K.L.B. Chang, Chitosan-catalyzed aggregation during the biomimetic synthesis of silica nanoparticles, Chemistry of Materials 18 (2006) 702–707.
[9] K.D. Demadis, A. Ketsetzi, K. Pachis, V.M. Ramos, Inhibitory effects of multicomponent, phosphonate-grafted zwitterionic chitosan biomacromolecules on silicic acid condensation, Biomacromolecules 9 (2008) 3288–3293.
[10] T. Witoon, M. Chareonpanich, J. Limtrakul, Effect of acidity on the formation of silica–chitosan hybrid materials and thermal conductive property, Journal of Sol–Gel Science and Technology 51 (2009) 146–152.
[11] T. Witoon, M. Chareonpanich, J. Limtrakul, Size control of nanostructured silica using chitosan template and fractal geometry: effect of chitosan/silica ratio and aging temperature, Journal of Sol–Gel Science and Technology 56 (2010) 270–277.
[12] T. Witoon, S. Tepsarn, P. Kittipokin, B. Embley, M. Chareonpanich, Effect of pH and chitosan concentration on precipitation and morphology of hierarchical porous silica, Journal of Non-Crystalline Solids 357 (2011) 3513–3519.
[13] G.B. Alexander, R.K. Iler, Determination of particle sizes in colloidal silica, Journal of Physical Chemistry 57 (1953) 932–934.
[14] R.K. Iler, Chemistry of Silica, John Wiley & Sons, New York, 1979.
[15] C.J. Brinker, G.W. Scherer, Sol–Gel Science: The Physics and Chemistry of Sol–Gel Processing, Academic Press, London, 1990.
[16] K.D. Demadis, K. Pachis, A. Ketsetzi, A. Stathoulopoulou, Bioinspired control of colloidal silica *in vitro* by dual polymeric assemblies of zwitterionic phosphomethylated chitosan and polycations or polyanions, Advances in Colloid and Interface Science 151 (2009) 33–48.